

# Efficient Fusion of Sparse and Complementary Convolutions for Object Recognition and Detection

Chun-Fu (Richard) Chen<sup>1</sup>, Quanfu Fan<sup>1</sup>, Marco Pistoia<sup>1</sup>, Gwo Giun (Chris) Lee<sup>2</sup>

<sup>1</sup>IBM T.J. Watson Research Center, {chenrich, qfan, pistoia}@us.ibm.com

<sup>2</sup>National Cheng Kung University, clee@mail.ncku.edu.tw

**Abstract.** We propose a new method for exploiting sparsity in convolutional kernels to create compact and computationally efficient convolutional neural networks (CNNs). Our approach is based on hand-crafted sparse kernels that are spatially complementary, allowing for an effective combination of them to represent more complex but discriminative kernels in an efficient way. Based on this, we develop a module that can be used to replace a convolutional kernel of any size greater than 1. We integrate such a module into various existing CNN models and conduct extensive experiments to demonstrate the effectiveness of our proposed approach on image classification as well as object localization and detection. The experiments validate the adaptability of the proposed method. For classification and localization, the proposed approach achieves competitive or better performance than the baselines and related works for various networks while providing lower computational costs and fewer parameters (on average, a  $2 - 3\times$  reduction of convolutional parameters and a  $2 - 4\times$  speedup in computation). On the other hand, our approach leads to a VGG16-based Faster RCNN detector that is  $12.4\times$  smaller and about  $3\times$  faster than the baseline.

**Keywords:** CNN, sparse kernels, compression, classification and detection

## 1 Introduction

Object recognition has made significant progress recently with convolutional neural networks (CNNs) [1,2,3]. To achieve competitive performance, CNNs need to increase their sizes substantially with deep architectures. Unfortunately, the increased complexity of these models in computation and structure makes it difficult to train them and deploy them to real-time visual analysis or resource-constrained applications.

There have been significant research efforts in making CNN models smaller and faster. One research line aims to develop extremely compact network architectures for mobile devices with limited computational power, e.g., SqueezeNet [4],

MobileNet [5] and ShuffleNet [6]. Another direction focuses on model compression to reduce parameter redundancy in pre-trained models. The techniques explored in the literature include vector quantization [7], low-rank approximation [8,9,10,11,12], kernel sparsification [13,14,15,16] and network thinning [17,18], just to name a few. These approaches demonstrate impressive ability to reduce model size and computational time without compromising much on classification accuracy. Nonetheless, these models have been only evaluated on classification, thus it's less clear how the significant compression affects their adaption capability for other vision tasks such as object detection.

In this work, we propose an efficient approach based on kernel sparsification to reduce parameter redundancy in CNNs. Unlike other model compression techniques that learn sparse representations, our approach exploits spatial complementary (*SC*) kernels designed by hand. The *SC* kernels, recently proposed by Fan *et al.* [19], are paired sparse kernels that spatially complement each other by having zero weights either at the even or odd indices of a full kernel (see Section 3 for details). A nice property of the *SC* kernels is that, while each of them only sees part of the receptive field, a spatial join of them covers the entire field. This allows for an effective combination of them to enhance feature representation for more complex kernels. The approach in [19] combines the *SC* kernels by *sequential filtering*, which alternatively stacks them vertically within a model, in a similar spirit to separate filtering [12]. Nonetheless, the gain from such a combination is only moderate, with a reduction of convolutional parameters by approximately  $1.5\times$ .

To address such a limitation, we explore two ways in this paper to fuse the sparse kernels. The first one, namely *pairwise kernel fusion*, approximates a full convolution by fusing the paired *SC* features in parallel. As illustrated in Fig. 1, such a method has the advantage over sequential filtering of covering all the pixels in the receptive field, potentially reserving better local image details in the feature representation, as validated in the object localization and detection tasks in the experiments. Note that the computational overhead of this fusion is negligible compared to the cost of convolution. The composite features, along with the *SC* features themselves, are further joined together by a  $1 \times 1$  convolution in the channel dimension, which is referred to as *channel-wise kernel fusion*. Based on these two types of kernel fusions, We design and implement a module that can be used to instantiate any popular CNN architecture (See more details in Section 3). As shown later, the pairwise fusion can greatly strengthen the following channel-wise kernel fusion, thus resulting in powerful sparse feature representations with less base kernels and more compression.

Another motivation behind our design is that the regular sparse patterns in the *SC* kernels make it easy to map them to various computing platforms without much effort, thus can result in high throughput. On the other hand, previous approaches based on sparsity learning such as [13,14,15] could lead to performance degradation as more overheads are required to solve the irregularity in the learned sparse representation.

**Table 1.** Comparison with related works.

Related works	Key features	Orthogonality to <i>scFusion</i>
[7,12,11,10,13,20]	Low-rank approximation	Y
[21,22,9]	Low-rank kernels	N
[14,13]	Random sparsification	Y
[15,8,23,19]	Structural sparsification	Y
[24,4]	Mixed-rank kernels with channel-wise kernel fusion	Y
[16,17,18]	Network thinning	Y
Proposed	<i>scFusion</i>	–

The contributions of our work are three-fold. First, we propose an efficient but powerful sparse feature representation of CNNs and demonstrate its applicability on various CNN architectures. Second, we validate the superior adaptability our approach to several vision tasks including image classification, object localization and detection through extensive experimentation. Finally, we show that with our proposed approach we can achieve a faster-RCNN detector, which is up to  $3\times$  faster and  $12.4\times$  smaller than the baseline while staying competitive in performance.

## 2 Related Works

A great number of approaches have been proposed to reduce parameter redundancy and computational complexity in CNN models. We highlight some works most relevant to ours in Table 1. Below we provide a detailed review of the related works.

**Low-rank Approximation** factorizes learned kernels into low-rank kernels or directly deploys hand-crafted low-rank kernels [7,9,11,12,13,21,22]. Factorization-based approaches decompose high-rank kernels in a pre-trained model into multiple low-rank kernels [7,11,12,13,10,20]. Such techniques include principal component analysis, singular value decomposition, data-driven low-rank approximation or non-linear approximation. On the other hand, hand-crafted low-rank kernels allow for training a network from scratch [9,21,22]. Approaches in this category sequentially cascade low-rank kernels to approximate a full kernel, for instance, stacking two 1-D kernels to approximate one 2-D kernel. However, the information lost in the low-rank kernels may be challenging for these approaches to recover. Our approach overcomes this issue by exploiting sparse and complementary kernels for feature representation. Furthermore, most of these approaches are orthogonal to our work, so potentially we can apply them to further compress our models.

**Kernel Sparsification** learns sparsity by group regularization [8,13,14,15]. Those approaches usually require a pre-trained model and then use a regularizer

to obtain random or structural sparsity in the trained kernels. Re-training is needed for these approaches to recover performance. The sparsity is learned based on a random or structural weight regularizer, which forces a group of weights to be close to zeros, and then pruning those group of weights. These approaches achieve high model compression rates on fully-connected layers which contain the most parameters of a model. One big limitation of these approaches is that they usually require a dedicated computing platform due to random sparsity. This could lead to insignificant speedups. Furthermore, an overhead with random sparsity is that an additional table or a compressed representation is needed to record the non-zero positions. Our approach does not have such an issue as the sparse kernels used in our approach are highly structured, and implementation of such kernels is trivial. Moreover, those approaches can be deployed on top of our approach to have an even more compact model.

**Mixed-rank Kernels with Channel-wise Kernel Fusion** groups kernels of different ranks in the channel dimension [4,24]. Ioannou *et al.* [24] propose to mix two 1-D kernels ( $-$  and  $|$  shape) and one optional 2-D kernel for feature representation. Nonetheless, they use non-complementary kernels which are too sparse to extend to large kernel size. In [4], Iandola *et al.* further propose to mix  $1 \times 1$  and  $3 \times 3$  kernels together and combine them by a  $1 \times 1$  filter. Our approach enhances their work by fusing sparse and complementary kernels to enrich feature representations.

**Network Thinning** is an approach to remove multiple kernels of a convolutional layer to thin a CNN model. This approach uses a pre-trained model with a large amount of data to measure the importance of each kernel and discarding unimportant kernels; then, a re-training is required to recover its performance [16,17,18]. Our approach can be beneficial with this approach to further compress our model since the slimming approach is applicable to any trained models.

More recently there are some attempts to explore model compression through knowledge distillation [25,26,27]. While this is a promising direction, most of the works have not been tested on large datasets such ImageNet yet.

### 3 Our Approach

In this section, we develop a compact module based on *SC* kernels, which can be used to approximate a full kernel of any size except  $1 \times 1$  in a CNN model. Different from [19], which stacks *SC* kernels sequentially to form a sparse representation, our approach combines them pairwise in an efficient way to enhance the feature representation. We first introduce the *SC* kernels briefly and then further differentiate our approach from that in [19].

#### 3.1 Base Kernels for Sparse Representation

*SC* kernels are defined as a pair of sparse kernels that spatially complement each other. The base kernels proposed in [19] are the simplest form with regular

sparse patterns. These kernels, denoted by  $\mathbf{W}_{\text{even}}$  and  $\mathbf{W}_{\text{odd}}$  respectively, can be mathematically expressed by,

$$\begin{aligned} W_{\text{even}_{i,j,c,n}} &= 0, \text{ if } (j \times k + i) \bmod 2 \neq 0 \\ W_{\text{odd}_{i,j,c,n}} &= 0, \text{ if } (j \times k + i) \bmod 2 \neq 1 \text{ and } (j \neq \lfloor k/2 \rfloor \text{ and } i \neq \lfloor k/2 \rfloor), \end{aligned} \quad (1)$$

where  $(i, j)$  specifies the spatial location of a cell in a kernel,  $k$  is the kernel size,  $c$  is the channel index and  $n$  denotes the kernel index. Note that the center point is not forced to be zero for either  $\mathbf{W}_{\text{odd}}$  or  $\mathbf{W}_{\text{even}}$ . This is because this location often carries a large weight, which is better not overlooked [19]. According to Eq. 1, *SC* kernels can be extended to any kernel size larger than 1. Interestingly, for the  $3 \times 3$  kernel, the corresponding  $\mathbf{W}_{\text{even}}$  kernel is a  $\times$  shape and the  $\mathbf{W}_{\text{odd}}$  kernel is a  $+$  shape.

*SC* kernels are deterministic, meaning that there is no need to use an index table to store their sparse patterns in memory. This is a big advantage over many other sparse representation such as [13], [15] and [14]. Such a simple form also provides the regularity in computation, enabling most of computing platforms to increase the throughput without much effort.

Not that the  $1 \times 3$  and  $3 \times 1$  kernels used in [24] can be considered as a special type of deterministic sparse kernels, but they are not spatially complementary. Dilated convolution [20] is another type of sparse representation, It expands the kernel size by filling the empty positions with zeros, so it is structurally different from *SC* kernels. Dilated convolution is usually used to approximate large-size kernels, and mostly applied to semantics segmentation [23].

### 3.2 Fusion of *SC* Kernels

Sequential filtering stacks two or more small kernels in sequence to represent a larger one. This idea has proven effective for decreasing the number of parameters and computations in CNN models such as VGG [2]. Recently, channel-wise kernel fusion has been used in approaches like [4,24] to group kernels of different shapes across channels. To take advantage of the complement property of our base kernel, we propose to join them spatially at the same convolutional layer to approximate the response of a full kernel.

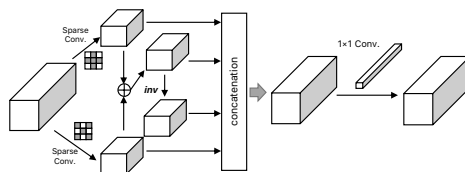


**Fig. 1.** Our proposed module (*scFusion*). Two sparse base kernels with complementary patterns are applied in parallel to extract features, which are joined together with two linear operations, *addition* and *inverse*. A subsequent  $1 \times 1$  filter further linearly combines the sparse features as well as the joint features.

Our idea is illustrated in Fig. 1. First, we apply the *SC* kernels with the input in parallel to extract the features in different phases to assure one of each sparse kernel covering partial receptive fields. We then combine them pairwise by linear operations such as *addition* and *inverse* (*pairwise kernel fusion*) to approximate the features with full receptive field. The responses of the *SC* kernels, together with the fused responses, are subsequently concatenated and further combined by a  $1 \times 1$  filter to learn a more discriminative feature representation (*channel-wise kernel fusion*). Note that we introduce a non-linearity, like ReLU, before the channel-wise kernel fusion. This justifies the need for the pairwise fusion as otherwise theoretically it would make no difference due to the existence of channel-wise kernel fusion.

Two element-wise operations, *addition* and *inverse*, are used in our work for pairwise kernel fusion. Since two base kernels are spatially complemented each other, it is natural to add them together to represent a full kernel. This is not only efficient, but also effective as the *addition* operator regularizes the two base kernels to learn complementary features, which are consequently enriched when combined together. Inspired from the work of [28], we further negate the response of a kernel to simulate a symmetric kernel. This empowers *scFusion* in feature representation without introducing much computational overheads. Our design allows easy incorporation of additional operations; however, it is suggested by theoretic analysis that more linear combinations do not provide additional benefit. Our experiments also validate that these two simple operations are sufficient enough to provide good results.

The pairwise kernel fusion incurs almost no computation compared to the cost of full convolutions. Nonetheless, the full kernel approximations obtained from this combination strengthen the following channel-wise kernel fusion in feature representation. As shown later in the experiments, such enhancement is critical for our approach achieving good accuracy in scenarios when fewer base kernels are desired for more computational savings.

**Comparison with Sequential Filtering** There are a few advantages of our approach over sequential filtering adopted in [19]. Firstly, *scFusion* is more flexible, allowing for different ways to combine the *SC* kernels, as shown above. Secondly, simply summing up the *SC* kernels covers the entire receptive field without overlooking any pixels, thanks to the nice spatially complementary property of the filters. On the other hand, sequential filtering of the *SC* filters always results in a few pixels skipped in the convolution, as illustrated in Fig. 1. Finally, our design of *scFusion* enables more powerful sparse representations, but with fewer base kernels. As shown in the experiments, *scFusion* achieves significantly better savings in both computation and model size than [19] while performing better on all the evaluation tasks.

### 3.3 Theoretical Complexity Analysis

We provide a theoretical analysis of the complexity reduction of *scFusion* as compared to conventional convolution in FLOPs and parameter numbers. The complexity of *scFusion* is directly controlled by the number of each base kernels.

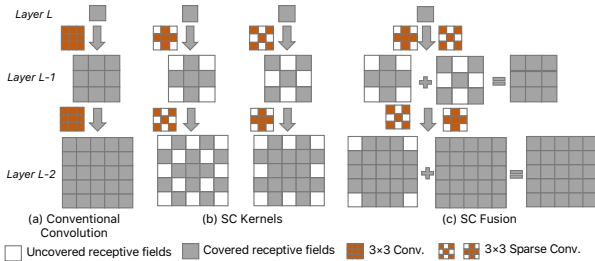


**Fig. 2.** Receptive fields in different convolutional methods. (a) Conventional convolution. (b) Two cases of *SC* kernels [19]. (c) *scFusion*. The *SC* kernels skip some pixels in the receptive field due to sparse convolution while *scFusion* cover all the pixels like the conventional convolution.

For a convolutional layer  $L_i$  with kernel size  $h \times w$ , and number of kernels is  $N_i$ , for a given input tensor with  $C_i \times H_i \times W_i$  shape, the total computation is  $hwC_iN_iH_iW_i$ ; for *scFusion* with the same input tensor and output tensor size but only uses  $n_i$  kernels for each sparse kernel, it requires  $2 \times \lceil hw/2 \rceil C_i n_i H_i W_i + 4n_i N_i H_i W_i$ , where the second term comes from the channel-wise fusion (The input channels of  $1 \times 1$  convolution will be four times of the number kernels of one sparse convolution.). Hence, we derive the reduction ratio  $\rho_i$  of FLOPs as Eq. 2; furthermore, we define a complexity controlling parameter  $\alpha_i = N_i/n_i$  as the ratio of the total number of kernels  $N_i$  over the number of each base kernels  $n_i$  at the  $i^{th}$  layer. The  $\rho_i$  would be proportional to  $\alpha_i$ ; thus, it is easy to control the complexity of *scFusion*. Moreover, despite the theoretical speedup, Liu *et al.* proved that current GPU architecture can take the advantages over deterministic sparse pattern in a convolutional layer even though the highly-optimized Winograd algorithm in CUDNN [29]. The reduction ratio of parameter numbers can be derive in the same way.

$$\begin{aligned}
 \rho_i &= \frac{hwC_iN_iH_iW_i}{2 \times \lceil hw/2 \rceil C_i n_i H_i W_i + 4n_i N_i H_i W_i} \\
 &= \frac{hwC_iN_i}{2 \times \lceil hw/2 \rceil C_i n_i + 4n_i N_i} \tag{2} \\
 &= \frac{\alpha_i hw}{(2 \times \lceil \frac{hw}{2} \rceil + 4 \frac{N_i}{C_i})}.
 \end{aligned}$$

For example, in the case of a  $3 \times 3$  kernel and  $\frac{N_i}{C_i} = 2$  (a typical configuration for a CNN model),  $\rho_i$  is  $2 \times$  when  $\alpha = 4$ . When  $\alpha = 8$ ,  $\rho_i$  is significantly increased to  $4 \times$ . Hence, by setting  $\alpha$  to different values, our approach offers a flexible way to trade off between algorithmic performance and model complexity.

**Table 2.** Classification accuracy on CIFAR-10 of our models.

	Model	Top-1 Acc.	FLOPs ↓	Params ↓ (Total)
3-Conv-NN [34]	baseline	81.71%	—	—
	<i>scFusion-2</i>	<b>82.06%</b>	1.29×	1.40×
	<i>scFusion-4</i>	80.90%	2.54×	2.41×
NIN [35]	baseline	<b>92.29%</b>	—	—
	<i>scFusion-2</i>	92.04%	1.15×	1.38×
	<i>scFusion-4</i>	91.91%	2.04×	2.55×
ResNet-32 [36]	baseline	93.98%	—	—
	<i>scFusion-2</i>	<b>94.37%</b>	1.26×	1.25×
	<i>scFusion-4</i>	93.16%	2.45×	2.39×
ResNet-164 [37]	baseline	94.58%	—	—
	<i>scFusion-2</i>	<b>95.21%</b>	1.28×	1.27×
	<i>scFusion-4</i>	94.89%	2.56×	2.51×
DenseNet-40 [3]	baseline	93.89%	—	—
	<i>scFusion-2</i>	95.01%	1.53×	1.60×
	<i>scFusion-4</i>	<b>94.60%</b>	2.37×	2.62×

## 4 Experimental Results

We conducted extensive experiments below to validate the effectiveness of our proposed approach on image classification, and compared our models with other works of sparse modeling. We also demonstrated the adaption capability of our approach on another two vision tasks, object localization and object detection.

### 4.1 Classification

**Experimental Setup** We first evaluated our proposed approach on classification using CIFAR-10 [30] and ImageNet [31]. A sparse version of a reference CNN model is created by replacing all the convolutional layers with the *scFusion* modules described in Section 3. The number of input and output channels in a *scFusion* module is set to the exactly the same as that of the reference model for fair comparison. We chose the Caffe deep learning framework for model training and test [32].

We trained all the models from scratch using the identical hyper-parameters of the baseline networks such as momentum and weight decay, initial learning rate, batch size, etc. Training data are augmented with horizontal flipping and mean subtraction for AlexNet and additional scale and aspect ratio augmentation [33] for VGG-16 and ResNet-50. All training details can be found in supplementary.

For clarity, a model studied below is named as *scFusion- $\alpha$*  where  $\alpha \in \{2, 4, 8\}$  is the reciprocal of the complexity controlling parameter defined in Section 3.3. We applied the same  $\alpha$  for all the convolutional layers in our experiments. In what



**Table 3.** Classification results of *scFusion* on ImageNet and other approaches. **Blob** numbers indicate the best performance among all models except for the baseline.

Network	Top-1 Acc.	Top-5 Acc.	FLOPs ↓	Params ↓ (Conv)	Params ↓ (Total)
Original [1]	57.72%	80.46%	–	–	–
<i>scFusion-4</i> (ours)	<b>58.64%</b>	<b>81.56%</b>	1.88×	2.43×	1.02×
<i>scFusion-8</i> (ours)	54.35%	78.56%	2.63×	3.24×	1.03×
<i>SC</i> kernels [19]	56.44%	79.73%	1.74×	1.74×	1.01×
Liu [13]	55.00% <sup>†</sup>	N/A	N/A	N/A	N/A
Zhou [8]	55.42%	N/A	N/A	N/A	2.23×*
Deep Compression [14]	57.23%	80.30%	N/A	2.69×*	9×*
SSL-2 [15]	57.57%	N/A	N/A	2.84×*	1.03×*
Molchanov [16]-A	N/A	76.00%	1.88×	N/A	N/A
Molchanov [16]-B	N/A	72.50%	2.82×	N/A	N/A
Original [2]	70.94%	89.91%	–	–	–
<i>scFusion-4</i> (ours)	<b>71.52%</b>	<b>90.25%</b>	2.40×	1.60×	1.04×
<i>scFusion-8</i> (ours)	69.90%	89.22%	4.64×	3.21×	1.08×
<i>scFusion-8</i> w/ [14] (ours) <sup>‡</sup>	68.83%	88.79%	4.64×	3.21×	11.82×*
<i>SC</i> kernels [19]	69.20%	88.91%	1.56×	1.56×	1.04×
ThiNet-Conv [18]	69.80%	89.53%	3.23×	N/A	1.05×
Deep Compression [14]	68.83%	89.09%	N/A	3.06×	13×*
GreBdec [20]	68.75%	89.06%	N/A	4.50×	14.22×*
Molchanov [16]-A	N/A	87.00%	1.33×	N/A	N/A
Molchanov [16]-B	N/A	84.50%	1.91×	N/A	N/A
Original [36]	<b>75.21%</b>	<b>92.24%</b>	–	–	–
<i>scFusion-4</i> (ours)	74.27%	91.96%	1.23×	1.21×	1.21×
<i>scFusion-8</i> (ours)	73.53%	91.52%	1.50×	1.44×	1.44×
ThiNet-70 [18]	72.04%	90.68%	1.58×	1.51×	1.51×

<sup>†</sup>: Accuracy is interpreted from their figure.

\*: Derived based on number of zeros but indexed table is **not** included.

<sup>‡</sup>: Apply deep compression on FC layers only.

follows, the experimental results are reported using top-1 and top-5 accuracies as well as reductions in FLOPs and parameters.

**Results on CIFAR-10** On CIFAR-10, we tested our approach with several CNNs including simple architectures such as 3-Conv-NN [34] and NIN [35] as well as more sophisticated ones such as ResNet [36],[37] and DenseNet [3]. Both  $3 \times 3$  and  $5 \times 5$  kernels are sparsified in these models, suggesting that *scFusion* is effective regardless of kernel size.

Table 2 lists the results of different CNNs. Our approach (*scFusion-4*) performs comparably against or better than the baseline models under different architectures while providing over  $2\times$  savings of model parameters and FLOPs. This clearly demonstrates that *scFusion* is capable of providing not only efficient but effective feature representations for image classification.

**Results on ImageNet** On ImageNet, we evaluated our proposed approach with some popular CNNs including AlexNet [1], VGG-16 [2] and ResNet [36]. In all these networks, we keep the first convolutional layer dense since sparsifying the first convolutional layer leads to a slight performance drop; however, the first layer only accounts for a small portion of the parameters and computations, we keep it intact in our models.

The classification results of the models described above are summarized in Table 3. Overall our approach demonstrates competitive performance against the AlexNet and VGG-16 baselines. *scFusion-4* yields better top-1 and top-5 accuracies than the baselines while giving reasonable savings on model parameters and FLOPs. On the other hand, when fewer base kernels (e.g.  $\alpha = 8$ ) are used, *scFusion-8* gains a significant reduction of over  $4\times$  in FLOPs and over  $3\times$  in convolutional parameters, with only about 1% drop on top-1 accuracy for VGG-16.

ResNet has a compact structure heavily adopting  $1 \times 1$  convolutions, thus it is challenging to further prune parameters on this network architecture. Despite this, our approach (*scFusion-8*) still achieves a reduction of parameters and FLOPs by  $1.5\times$  on ResNet-50, with roughly a top-1 accuracy drop of 1.5%.

**Comparison With Other Approaches** We compared our approach with some recently developed techniques of model compression by sparse kernel representation [8,13,14,15,16,19,20]. Among them, the work of [14] is based on sparsity pruning while other approaches all learn sparsity in kernels via group regularization [8,13,15]. We also include in our evaluation one new method based on network thinning, ThiNet [18]. This approach focuses on filter-level pruning, which removes an entire filter if it’s insignificant.

As indicated by Table 3, our approach outperforms all others while delivering comparable savings in terms of convolutional parameters and computations. Especially, on VGG16, *scFusion-8* achieves a significantly better FLOPs reduction than any other approach in comparison. On ResNet-50, our approach results in a similar gain of computation and parameter savings to ThiNet-70, but is 1.5% point better on top-1 accuracy. The notable performance gap between *scFusion* and *SC* kernels [19] strongly suggests that our fusion methodology is superior to sequential filtering.

Approaches like [8] and [14] perform sparsification on the entire network architecture, so they benefit greatly from pruning the FC layers, which leads to a much higher reduction rate with regards to the total model size. Since our approach is orthogonal to many other model compression techniques, we applied the technique proposed in [14] to further prune the FC layers in our VGG-16-based *scFusion-8* model. As shown in Table 3, this gives rise to a total reduction of almost  $12\times$  with only a slight drop in accuracy.

**Analysis on Pairwise Fusion.** To understand the contribution of each operation in the pairwise kernel fusion, we ran a control experiment on CIFAR-10 by doing *no-fusion* (*scConv*) and *addition* only (*scFusion<sub>add</sub>*), and compared the results with those of *scFusion* in Table 4. Clearly, by having two operations

**Table 4.** Top-1 Acc. of *scConv-4*, *scFusion<sub>add-4</sub>* and *scFusion-4* of different CNNs on the CIFAR-10 dataset.

Network	<i>scConv-4</i>	<i>scFusion<sub>add-4</sub></i>	<i>scFusion-4</i>
3-Conv-NN	78.31%	79.72%	<b>80.90%</b>
NIN	91.03%	91.11%	<b>91.91%</b>
ResNet-32	92.42%	92.95%	<b>93.16%</b>

**Table 5.** Top-1 Acc. of ResNet-32 network on the CIFAR-10 dataset.

Mixed-rank Kernels		Pairwise Kernel Fusion	
Non-complementary* [24]	Complementary	Non-complementary*	Complementary
93.22%	93.46%	94.05%	<b>94.37%</b>

\*: Two 1-D non-complementary kernels.  $\alpha = 2$  for all cases.

as our fusion approaches (*addition* and *inverse*), we can improve performance with a negligible computational load; furthermore, except for NIN, two operations can be considered as equal contributions for the performance improvement (similar accuracy improvement after adding one more fusion operator). Hence, the pairwise fusion enriches feature representation in an efficient way.

**Complementary v.s Non-complementary Kernels.** To validate that kernel complement is helpful, we substituted the *SC* kernels in our approach by a pair of non-complementary filters (e.g.  $1 \times 3$  and  $3 \times 1$  for  $3 \times 3$  kernels) used in [24]. In the meanwhile, we applied our base kernels to the approach in [24] as well. The baseline model is ResNet-32 in both cases. As shown in Table 5, the *SC* kernels demonstrate clear advantages over the non-complementary filters by showing more than 1% point accuracy improvement under both approaches. This also implies that pairwise fusion can also enhance feature representation even if kernels are not complemented.

## 4.2 Object Localization

To demonstrate the adaption capability of our approach to other vision tasks, we evaluated our approach on the object localization task in this section. The goal of object localization is to find the location of a single object in an image along with correct prediction.

Following the methodology used in [38], For VGG-16, we replaced the fully-connected layers of a VGG16-based *scFusion* model by global average pooling, adding another  $3 \times 3$  convolutional layer with 1,024 output channels after *conv5\_3*, and then fine-tuning the model using ILSVRC data. We then applied the same algorithm and parameters as used in [38] to localize an object based on the class attention map (CAM) for each of the top-5 predictions. Shown in Table 6 are the top-1 and top-5 localization errors on the validation and test sets of ILSVRC-2014, respectively.

As indicated by Table 6, on VGG-16, both *scFusion-4-GAP* and *scFusion-8-GAP* outperforms the baseline by a large margin. Our results are also better

**Table 6.** Localization errors on the ILSVRC-2014 validation and test sets.

Network	Dataset	Top-1 Error	Top-5 Error
VGG-16-GAP [38]	val.	57.20%	45.14%
VGG-16- <i>scFusion</i> -4-GAP		<b>51.88%</b>	<b>40.04%</b>
VGG-16- <i>scFusion</i> -8-GAP		53.89%	41.62%
GoogLeNet [38]		56.40%	43.00%
VGG-16- <i>scFusion</i> -4-GAP	test	—	<b>37.3%</b>
VGG-16- <i>scFusion</i> -8-GAP		—	41.8%
GoogLeNet [38]		—	42.9%
Backprop [39]		—	46.4%

than GoogLeNet, the best results reported in [38]. The localization performance of our approach seems to suggest that *scFusion* can preserve local image details well, which is confirmed in the object detection task later.

We further evaluated our approach on the ILSVRC-2014 test set. Our approach consistently produces better results than GoogLeNet. On the other hand, our approach does object localization in a weakly supervised way, but still outperforms Backprop [39], a fully supervised approach for the localization task.

To understand why our approach is effective at object localization, we take a closer look at the two examples in Figure 3, which illustrate the contribution of each component of the *scFusion* module ( $\mathbf{W}_{\text{even}}$ ,  $\mathbf{W}_{\text{odd}}$ , fusion-add, fusion-inv). From them, we can learn a) Fusion operation, either addition or inverse, learns similar salient parts of an object, indicating they provide strong approximation of full kernels; b)  $\mathbf{W}_{\text{even}}$  and  $\mathbf{W}_{\text{odd}}$  activates different parts of an object, indicating they contribute supplementally to object classification; and c) combining all of the items leads to stronger activation than the original model.

### 4.3 Object Detection

In this section, we validated our approach on the object detection task. We used our *scFusion* models as feature extractors and trained Faster-RCNN [40] detectors on the PASCAL VOC [41] and MS COCO dataset [42]. For PASCAL

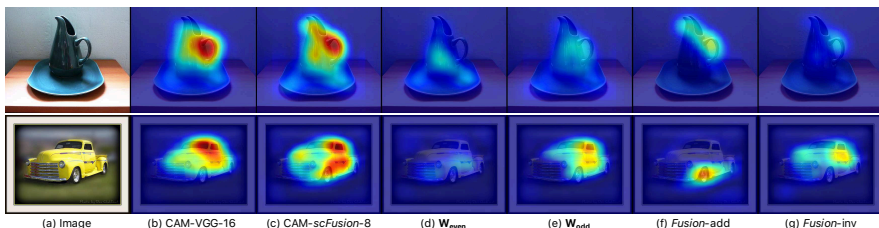


**Fig. 3.** Class attention map from each component in *scFusion*-8 of VGG-16. (b) the baseline VGG-16-GAP, (c) the *scFusion*-8 and (d)-(g) denotes the CAM maps from each component.

**Table 7.** Object detection results on the MS COCO test2015-dev dataset.

Detector	Ave. Precision IoU	
	0.5:0.95	0.5
VGG-16 [43]	21.9	42.7
<i>scFusion-8</i> (ours)	<b>22.8</b>	<b>43.3</b>

**Table 8.** Object detection results on the VOC2007 test set.

Detector	Accuracy (mAP)
baseline	62.2
<i>scFusion-4</i>	<b>62.3</b>
<i>SC</i> kernels [19]	61.1
Deep Compression [14]	54.3
SSL-2 [15]	58.5
<hr/>	
baseline [40]	73.2
<i>scFusion-8</i> (ours)	<b>73.9</b>
<i>scFusion-8-GAP</i> (ours)	40.9
<i>SC</i> kernels [19]	73.1
ThiNet-Conv-GAP [18]	34.2

VOC, we combined the training and validation sets of VOC2007 and VOC2012 as training data, and then evaluated the detector on the VOC2007 test set. For MS COCO, we used the 2014 train + val35k as suggested in [43] for training and test2015-dev for testing.

**Detection Results on VOC2007 and MS COCO** We include 4 other model compression approaches in our evaluation, including Deep Compression [14], SSL-2 [15], ThiNet [18], and *SC* kernels [19]. They were also used in the evaluation of the classification task in Section 4.1. Deep compression [14], SSL-2 [15] and *SC* kernels [19] are based on sparse representation. When training faster RCNN with these models, we disabled updating of any zero weight from them except ThiNet [18] in order to maintain their original sparsity. With ThiNet, we append the classification and regression layers in faster RCNN directly to the GAP layer of the classification model. For fair comparison, all detectors were trained and tested at the default settings given by [44].

Table 8 lists the results of object detection from all the approaches on the VOC2007 test set. Our approach is slightly better than the baseline while outperforms all the others in comparison. Note that ThiNet [18] yields an extremely low accuracy on detection. We speculate that this has to do with the change in this model which substitutes the FC layers by a GAP layer. To confirm this, we trained a faster-RCNN detector with our *scFusion-8-GAP* model, which undergoes a similar structural modification. While doing better, this detector only leads to an accuracy of 40.9, which is still far beyond satisfactory.

Table 7 shows the detection results on the more challenging MS COCO dataset. Again, our approach achieves better performance than the VGG16 baseline.

**Table 9.** Object detection results on VOC2007 test set.

Detector	Test Scale	Training Scale	Accuracy (mAP)	Model (MB)	Speed (ms)
VGG-16 baseline [40]	600	[600]	73.2	522	275
<i>scFusion</i> -8	600	[600]	73.9	475	202
<i>scFusion</i> -8	512	[256,512,768]	<b>74.4</b>	475	126
<i>scFusion</i> -8 (sp2-fc512)	512	[256,512,768]	73.4	<b>42</b>	<b>93</b>

sp2: sparse ROI pooling with even-indexed features. fc512: the size of FC layer is reduced to 512.

**Efficient and Compact Detectors** We benchmarked our *scFusion*-based detector on a machine with a Intel Xeon 10-cores CPU and a NVIDIA Tesla K80 GPU card. As shown in Table 9, our approach yields a speedup of  $1.4\times$  in computation. To further improve its efficiency, we trained a detector with three scales with the same image height and width [256 $\times$ 256, 512 $\times$ 512, 768 $\times$ 768] and tested the detector on a scale of 512 $\times$ 512 rather than the default scale of 600 $\times$ 1000 in faster RCNN. With this, the detector sees a significant speedup of more than  $2\times$  while achieving a better accuracy than the model trained on a single scale and larger resolution.

Since *scFusion* is only applied to convolution layers, a remaining issue for a faster-RCNN detector based on our approach is the size of the model, which is dominated by the parameters from the FC layers. To build a more compact detector, we reduced the number of nodes on the FC layers from 4096 to 512, similar to what’s done in [19]. As can be seen from Table 9, doing so leads to a very compact model as small as 42M, which sees another  $1\times$  speedup over the *scFusion*-8 model trained with multiple scales. Overall, this detector is  $12.4\times$  smaller and  $3\times$  faster in inference than the VGG16-based faster RCNN while staying competitive in performance. We expect that such well-performed but tiny detectors have important applications to resource-constrained devices such as mobile phones and FPGAs.

## 5 Conclusion

We have presented a new approach for creating computationally efficient CNN models with sparse kernel representation. Our approach benefits from the base kernels that are sparse and complementary for extracting distinct and discriminative features. This enables us to combine base kernels to represent more complex kernels to enrich feature representation. The combination is simple but efficient to improve performance, and the presented fusion approaches are almost cost-free. We have integrated our approach into various existing CNN models and conducted extensive experiments to demonstrate the effectiveness of the approach for multiple tasks, like visual recognition, object localization and object detection, which validates the adaptability of the proposed method is effective. For classification and localization, *scFusion* always outperforms the baselines and related work for all networks; on the other hand, our detector is  $3\times$  faster and  $12.4\times$  smaller than the baseline with competitive performance.

## References

1. Krizhevsky, A., Sutskever, I., Hinton, G.E.: Imagenet classification with deep convolutional neural networks. *Advances in Neural Information Processing Systems (NIPS)* (2012) 1097–1105
2. Simonyan, K., Zisserman, A.: Very Deep Convolutional Networks for Large-Scale Image Recognition. In: *International Conference on Learning Representations (ICLR)*. (2015)
3. Huang, G., Liu, Z., van der Maaten, L., Weinberger, K.Q.: Densely Connected Convolutional Networks. In: *The IEEE Conference on Computer Vision and Pattern Recognition (CVPR)*. (July 2017)
4. Iandola, F.N., Moskewicz, M.W., Ashraf, K., Han, S., Dally, W.J., Keutzer, K.: SqueezeNet: AlexNet-level accuracy with 50x fewer parameters and <0.5MB model size. In: *International Conference on Learning Representations (ICLR)*. (2016)
5. Howard, A.G., Zhu, M., Chen, B., Kalenichenko, D., Wang, W., Weyand, T., Andreetto, M., Adam, H.: MobileNets: Efficient Convolutional Neural Networks for Mobile Vision Applications. *CoRR* [abs/1704.04861](#) (2017)
6. Zhang, X., Zhou, X., Lin, M., Sun, J.: ShuffleNet: An Extremely Efficient Convolutional Neural Network for Mobile Devices. *CoRR* [abs/1707.01083](#) (2017)
7. Denton, E.L., Zaremba, W., Bruna, J., LeCun, Y., Fergus, R.: Exploiting Linear Structure Within Convolutional Networks for Efficient Evaluation. In: *Advances in Neural Information Processing Systems (NIPS)*. (2014)
8. Zhou, H., Alvarez, J.M., Porikli, F.: Less is more: Towards compact cnns. In: *European Conference on Computer Vision (ECCV)*. (2016)
9. Sun, Z., Ozay, M., Okatani, T.: Design of Kernels in Convolutional Neural Networks for Image Classification. In: *European Conference on Computer Vision (ECCV)*. (2016)
10. Kim, Y.D., Park, E., Yoo, S., Choi, T., Yang, L., Shin, D.: Compression of Deep Convolutional Neural Networks for Fast and Low Power Mobile Applications. In: *International Conference on Learning Representations (ICLR)*. (2016)
11. Zhang, X., Zou, J., Ming, X., He, K., Sun, J.: Efficient and Accurate Approximations of Nonlinear Convolutional Networks. In: *IEEE Conference on Computer Vision and Pattern Recognition (CVPR)*. (2015)
12. Jaderberg, M., Vedaldi, A., Zisserman, A.: Speeding up convolutional neural networks with low rank expansions. In: *Proceedings of the British Machine Vision Conference*. (2014)
13. Liu, B., Wang, M., Foroosh, H., Tappen, M., Pensky, M.: Sparse convolutional neural networks. In: *IEEE Conference on Computer Vision and Pattern Recognition (CVPR)*. (2015)
14. Han, S., Mao, H., Dally, W.J.: Deep Compression: Compressing Deep Neural Network with Pruning, Trained Quantization and Huffman Coding. In: *International Conference on Learning Representations (ICLR)*. (2015)
15. Wen, W., Wu, C., Wang, Y., Chen, Y., Li, H.: Learning Structured Sparsity in Deep Neural Networks. In: *Advances in Neural Information Processing Systems (NIPS)*. (2016)
16. Molchanov, P., Tyree, S., Karras, T., Aila, T., Kautz, J.: Pruning Convolutional Neural Networks for Resource Efficient Transfer Learning. In: *International Conference on Learning Representations (ICLR)*. (2017)
17. Liu, Z., Li, J., Shen, Z., Huang, G., Yan, S., Zhang, C.: Learning Efficient Convolutional Networks Through Network Slimming. In: *The IEEE International Conference on Computer Vision (ICCV)*. (October 2017)

18. Luo, J.H., Wu, J., Lin, W.: ThiNet: A Filter Level Pruning Method for Deep Neural Network Compression. In: The IEEE International Conference on Computer Vision (ICCV). (October 2017)
19. Fan, Q., Chen, C.F., Lee, G.G.: A sparse deep feature representation for object detection from wearable cameras. In: British Machine Vision Conference (BMVC). (2017)
20. Yu, X., Liu, T., Wang, X., Tao, D.: On Compressing Deep Models by Low Rank and Sparse Decomposition. In: The IEEE Conference on Computer Vision and Pattern Recognition (CVPR). (July 2017)
21. Mamalet, F., Garcia, C.: Simplifying ConvNets for Fast Learning. In: Artificial Neural Networks and Machine Learning (ICANN). (2012)
22. Szegedy, C., Vanhoucke, V., Ioffe, S., Shlens, J., Wojna, Z.: Rethinking the inception architecture for computer vision. In: IEEE Conference on Computer Vision and Pattern Recognition (CVPR). (2016)
23. Yu, F., Koltun, V., Funkhouser, T.: Dilated Residual Networks. In: The IEEE Conference on Computer Vision and Pattern Recognition (CVPR). (July 2017)
24. Ioannou, Y., Robertson, D.P., Shotton, J., Cipolla, R., Criminisi, A.: Training CNNs with Low-Rank Filters for Efficient Image Classification. In: International Conference on Learning Representations (ICLR). (2016)
25. Hinton, G., Vinyals, O., Dean, J.: Distilling the knowledge in a neural network. arXiv:1503.02531 (2015)
26. Sau, B.B., Balasubramanian, V.N.: Deep model compression: Distilling knowledge from noisy teachers. arXiv:1610.09650 (2016)
27. Gupta, S., Hoffman, J., Malik, J.: Cross modal distillation for supervision transfer. In: IEEE Conference on Computer Vision and Pattern Recognition (CVPR). (2016)
28. Shang, W., Sohn, K., Almeida, D., Lee, H.: Understanding and Improving Convolutional Neural Networks via Concatenated Rectified Linear Units. In: International Conference on Machine Learning (ICML). (2016)
29. Liu, X., Pool, J., Han, S., Dally, W.J.: Efficient sparse-winograd convolutional neural networks. In: International Conference on Learning Representations. (2018)
30. Krizhevsky, A., Hinton, G.: Learning multiple layers of features from tiny images. Technical report, University of Toronto (2009)
31. Russakovsky, O., Deng, J., Su, H., Krause, J., Satheesh, S., Ma, S., Huang, Z., Karpathy, A., Khosla, A., Bernstein, M., Berg, A.C., Fei-Fei, L.: ImageNet Large Scale Visual Recognition Challenge. *International Journal of Computer Vision (IJCV)* **115**(3) (2015) 211–252
32. Jia, Y., Shelhamer, E., Donahue, J., Karayev, S., Long, J., Girshick, R., Guadarrama, S., Darrell, T.: Caffe: Convolutional Architecture for Fast Feature Embedding. In: ACM International Conference on Multimedia (ACMMM). (2014) 675–678
33. Szegedy, C., Liu, W., Jia, Y., Sermanet, P., Reed, S., Anguelov, D., Erhan, D., Vanhoucke, V., Rabinovich, A.: Going deeper with convolutions. In: IEEE Conference on Computer Vision and Pattern Recognition (CVPR). (2015) 1–9
34. Krizhevsky, A.: cuda-convnet2. <https://code.google.com/p/cuda-convnet/>
35. Lin, M., Chen, Q., Yan, S.: Network In Network. *International Conference on Learning Representations (ICLR)* (2013)
36. He, K., Zhang, X., Ren, S., Sun, J.: Deep Residual Learning for Image Recognition. In: IEEE Conference on Computer Vision and Pattern Recognition (CVPR). (June 2016)
37. He, K., Zhang, X., Ren, S., Sun, J.: Identity Mappings in Deep Residual Networks. In: European Conference on Computer Vision (ECCV). (2016) 630–645



38. Zhou, B., Khosla, A., Lapedriza, A., Oliva, A., Torralba, A.: Learning Deep Features for Discriminative Localization. In: The IEEE Conference on Computer Vision and Pattern Recognition (CVPR). (June 2016)
39. K. Simonyan, A.V., Zisserman, A.: Deep inside convolutional networks: Visualising image classification models and saliency maps. In: International Conference on Learning Representations Workshop (ICLR). (2014)
40. Ren, S., He, K., Girshick, R., Sun, J.: Faster R-CNN: Towards Real-Time Object Detection with Region Proposal Networks. In: Advances in Neural Information Processing Systems (NIPS). (2015)
41. Everingham, M., Van Gool, L., Williams, C.K.I., Winn, J., Zisserman, A.: The Pascal Visual Object Classes (VOC) Challenge. International Journal of Computer Vision **88**(2) (June 2010) 303–338
42. Lin, T.Y., Maire, M., Belongie, S., Hays, J., Perona, P., Ramanan, D., Dollár, P., Zitnick, C.L.: Microsoft COCO: Common Objects in Context. In: European Conference on Computer Vision (ECCV). Springer International Publishing (2014) 740–755
43. Ren, S., He, K., Girshick, R., Sun, J.: Faster R-CNN: Towards Real-Time Object Detection with Region Proposal Networks. IEEE Transactions on Pattern Analysis and Machine Intelligence **39**(6) (June 2017) 1137–1149
44. Girshick, R.: py-faster-rcnn. <https://github.com/rbgirshick/py-faster-rcnn>
45. Qian, N.: On the momentum term in gradient descent learning algorithms. Neural Netw. **12**(1) (January 1999) 145–151

# Appendix

To facilitate reproducing our work, we provide details about the settings we used to train various models in our experiments. While the experimental settings can be different from datasets and models, we have applied identical hyper-parameters for the same network architecture for fair comparison.

## 6 Training Details for Classification Task

All networks were trained with the momentum optimizer [45] and the momentum is set to 0.9.

### 6.1 CIFAR-10

For 3-Conv-NN and NIN, the learning rate starts from 0.001 and then drops  $10\times$  at 50% and 75% epochs. The number of epochs is set to 120 and the batch size 100. Data augmentation includes pixel-wise mean subtraction and random horizontal flipping. During testing, only the pixel-wise mean subtraction is applied.

On the other hand, for ResNet-32, ResNet-164 and DenseNet-40, the learning rate starts from 0.1 and then drops  $10\times$  at 50% and 75% epochs. We trained 185 epochs for both ResNets and 300 epochs for DenseNet. The batch size is set to 128 for these three networks. During the training, 4 pixels are padded on four directions and then a  $32\times 32$  patch is cropped to increase its translation invariance. In Channel-wise mean and standard deviation normalization as well as random horizontal flipping are applied for data augmentation. In the testing phase, only the channel-wise mean and standard deviation normalization is used.

### 6.2 ImageNet

For AlexNet, we trained 90 epochs with a batch size of 256. The initial learning rate is 0.01, and drops  $10\times$  at the 20-th, 40-th, 60-th and 80-th epochs, respectively. We augmented data with horizontal flipping and pixel-wise mean subtraction.

For VGG-16 and ResNet-50, we trained 100 epochs with a batch size 256. The initial learning rate is 0.01 and 0.1 for VGG-16 and ResNet-50, respectively, and drops  $10\times$  at the 30-th, 60-th and 90-th epochs. We applied scale augmentation in [33], channel-wise mean and standard deviation normalization and random horizontal flipping.

For the *scFusion-8* on VGG-16 with the approach proposed in [14], we only fine-tuned the fully-connected layers. We deleted the weights whose absolute values are below 0.0001, and then kept them as zeros during fine-tuning. Afterwards, we trained 30 epochs with an initial learning rate of 0.001, which then drops  $10\times$  at the 20-th and 25-th epochs.

To measure the accuracy on the ImageNet validation dataset, we resized the shorter side of an image to 256 with its aspect ratio and then cropped a  $224\times 224$  center patch for evaluation.